Exponential-time differencing schemes for low-mass DPD systems

N. Phan-Thien[1,*], N. Mai-Duy[1,2], D. Pan[1] and B. C. Khoo[1],

[1]Department of Mechanical Engineering, Faculty of Engineering,
National University of Singapore, Singapore.
[2]Computational Engineering and Science Research Centre,
Faculty of Engineering and Surveying,
University of Southern Queensland, Toowoomba, QLD 4350, Australia.

Submitted to *Computer Physics Communications*, August 2012; revised, August 2013

*Corresponding author: E-mail nhan@nus.edu.sg, Telephone +65-6601-2054, Fax +65-6779-1459

Abstract

Several exponential-time differencing (ETD) schemes are introduced into the method of dissipative particle dynamics (DPD) to solve the resulting stiff stochastic differential equations in the limit of small mass, where emphasis is placed on the handling of the fluctuating terms (*i.e.,* those involving the random forces). Their performances are investigated numerically in some test viscometric flows. Results obtained show that the present schemes outperform the velocity-Verlet algorithm regarding both the satisfaction of equipartition and the maximum allowable time step.

Keywords: exponential-time differencing scheme, dissipative particle dynamics, stiff stochastic differential equation, overdamped systems

1 Introduction

The DPD method has emerged as a powerful computational tool for predicting hydrodynamic behaviour of complex-structure fluids like polymers and colloidal suspensions [1-9]. In the DPD method, a fluid is modelled by a set of particles that can move freely and the system conserves both mass and momentum. The stochastic differential equations governing the motion of a particle are given by

$$\frac{d\mathbf{r}_i}{dt} = \mathbf{v}_i, \tag{1}$$

$$m_i \frac{d\mathbf{v}_i}{dt} = \mathbf{F}_i, \tag{2}$$

where m_i, $\mathbf{r}_i$ and $\mathbf{v}_i$ represent the mass, position and velocity vector of a particle i, respectively; and $\mathbf{F}_i$ is the total force vector exerted on it, containing three parts

$$\mathbf{F}_i = \sum_{j=1, j\neq i}^{N} \left(\mathbf{F}_{ij,C} + \mathbf{F}_{ij,D} + \mathbf{F}_{ij,R} \right), \tag{3}$$

in which the sum runs over all other particles, denoted by j, within a certain cutoff radius r_c. The first term on the right is referred to as the conservative force (subscript C), the second dissipative force (subscript D) and the third random force (subscript R). These forces are usually given in

the forms

$$\mathbf{F}_{ij,C} = a_{ij} w_C \mathbf{e}_{ij}, \tag{4}$$

$$\mathbf{F}_{ij,D} = -\gamma w_D \left(\mathbf{e}_{ij} \cdot \mathbf{v}_{ij}\right) \mathbf{e}_{ij}, \tag{5}$$

$$\mathbf{F}_{ij,R} = \sigma w_R \theta_{ij} \mathbf{e}_{ij}, \tag{6}$$

where a_{ij}, γ and σ are constants reflecting the strengths of these forces; w_C, w_D and w_R the distance-dependent weighting functions; $\mathbf{e}_{ij} = \mathbf{r}_{ij}/r_{ij}$ a unit vector from particle j to particle i ($\mathbf{r}_{ij} = \mathbf{r}_i - \mathbf{r}_j$, $r_{ij} = |\mathbf{r}_{ij}|$); $\mathbf{v}_{ij} = \mathbf{v}_i - \mathbf{v}_j$ the relative velocity vector, and θ_{ij} a Gaussian white noise ($\theta_{ij} = \theta_{ji}$) with stochastic properties

$$\langle \theta_{ij} \rangle = 0, \tag{7}$$

$$\langle \theta_{ij}(t) \theta_{kl}(t') \rangle = \left(\delta_{ik}\delta_{jl} + \delta_{il}\delta_{jk}\right) \delta\left(t - t'\right), \text{with } i \neq k \text{ and } j \neq l. \tag{8}$$

It was shown [3] that the equilibrium and detailed balance of the system lead to the following constraints

$$w_D(r_{ij}) = \left(w_R(r_{ij})\right)^2, \tag{9}$$

$$k_B T = \frac{\sigma^2}{2\gamma}, \tag{10}$$

which relate the strength of the dissipative force to the strength of the random force through the definition of the thermodynamic temperature (the equipartition principle or fluctuation-dissipation theorem). A popular choice of the weighting functions is [4,5]

$$w_C(r_{ij}) = 1 - \frac{r_{ij}}{r_c}, \tag{11}$$

$$w_D(r_{ij}) = \left(1 - \frac{r_{ij}}{r_c}\right)^s. \tag{12}$$

where s is a constant ($s = 2$ and $s = 1/2$ are two typical values of s).

A considerable effort has been put into the development of numerical integration schemes to advance particles positions and velocities. Examples of integrators include the Euler-type, velocity-Verlet [5], self-consistent velocity-Verlet [10] and splitting [11] approaches, where the treatments

of the fluctuating part are all based on the Wiener process (Brownian motion), *i.e.,*

$$\Delta \mathbf{v}_i = \frac{1}{m_i} \sum a_{ij} w_C \Delta t \mathbf{e}_{ij} - \frac{1}{m_i} \sum \gamma w_D \left(\mathbf{e}_{ij} \cdot \mathbf{v}_{ij} \right) \Delta t \mathbf{e}_{ij} + \frac{1}{m_i} \sum \sigma w_R \Delta W_{ij} \mathbf{e}_{ij}, \tag{13}$$

with the autocorrelation defined as

$$\begin{aligned} \langle \Delta W_{ij}(\Delta t) \Delta W_{kl}(\Delta t) \rangle &= \int_0^{\Delta t} dt' \int_0^{\Delta t} dt'' \langle \theta_{ij}(t') \theta_{kl}(t'') \rangle \\ &= \left(\delta_{ik}\delta_{jl} + \delta_{il}\delta_{jk} \right) \Delta t. \end{aligned} \tag{14}$$

This leads to $\Delta W_{ij} = \xi_{ij}\sqrt{\Delta t}$, where ξ_{ij} is a random tensor with zero mean and unit variance, chosen independently for each pair of particles and each time step in the numerical integration process.

It should be noted that a DPD fluid is compressible in nature [12]. Reducing the mass of the particles is helpful in many cases - it reduces the Reynolds number, promotes incompressibility via an increase in the kinematic viscosity and speed of sound, and enhances the dynamic response of the fluid through an increase in the Schmidt number [13,14]. However, in the limit $m \to 0$, the corresponding DPD systems become stiff (this limit is also called the overdamped limit [15]). It can be seen that conventional explicit schemes are not efficient to solve such systems as the time step is limited by the stiff term. In this work, we introduce exponential-time differencing (ETD) integrators [16] into the DPD model. The stiff term in the deterministic part is treated in an exact manner, while the fluctuating part is handled according to the Ornstein-Uhlenbeck (O-U) process [17], which has a bounded variance. These schemes have the ability to handle very different time scales involved in an effective manner and deliver a convergent solution at large time steps. The paper is organised as follows. In Section 2, first-order and second-order stochastic ETD schemes for low mass DPD systems are presented. A modified version of the first-order stochastic ETD is also included. The verification is conducted by considering some geometric Brownian motions and viscometric flows in Section 3. Section 4 gives some concluding remarks.

2 Proposed integration schemes

Assuming a non-zero mass, the DPD velocity vector equation (2) can be rewritten as

$$\frac{d\mathbf{v}_i}{dt} = \frac{1}{m_i} a_{ij} w_C \mathbf{e}_{ij} - \frac{1}{m_i} \gamma w_D \left(\mathbf{e}_{ij} \cdot \mathbf{v}_{ij}\right) \mathbf{e}_{ij} + \frac{1}{m_i} \sigma w_R \theta_{ij} \mathbf{e}_{ij}. \tag{15}$$

For brevity, we express a component of the above vector equation in the form

$$\frac{du(t)}{dt} + cu(t) = a + b\theta\left(t\right), \tag{16}$$

where

$$u = \left(v_i\right)_\alpha, \tag{17}$$

$$c = \frac{1}{m_i} \sum_{j \neq i} \gamma w_D \left(\frac{\left(r_i\right)_\alpha - \left(r_j\right)_\alpha}{r_{ij}} \right)^2, \tag{18}$$

$$\begin{aligned} a = & - \frac{1}{m_i} \sum_{\beta=1,\beta\neq\alpha}^{3} \sum_{j \neq i} \gamma w_D \left(\frac{\left(r_i\right)_\beta - \left(r_j\right)_\beta}{r_{ij}} \right) \left(\frac{\left(r_i\right)_\alpha - \left(r_j\right)_\alpha}{r_{ij}} \right) \left(v_i\right)_\beta \\ & + \frac{1}{m_i} \sum_{j \neq i} \gamma w_D \left(\mathbf{e}_{ij} \cdot \mathbf{v}_j\right) \left(\frac{\left(r_i\right)_\alpha - \left(r_j\right)_\alpha}{r_{ij}} \right) + \frac{1}{m_i} \sum_{j \neq i} a_{ij} w_C \left(\frac{\left(r_i\right)_\alpha - \left(r_j\right)_\alpha}{r_{ij}} \right), \end{aligned} \tag{19}$$

$$b = \frac{1}{m_i} \sum_{j \neq i} \sigma w_R \left(\frac{\left(r_i\right)_\alpha - \left(r_j\right)_\alpha}{r_{ij}} \right), \tag{20}$$

in which the subscript $\alpha, \beta (= 1, 2, 3)$ is used to denote the αth component of the vectors in parentheses. It is noted that Groot and Warren [5] reported the following approximation for the stiff parameter

$$c = \frac{1}{3\tau}, \tag{21}$$

where

$$\frac{1}{\tau} = \gamma \sum_{j \neq i} w_{ij,D} \mathbf{e}_{ij} . \mathbf{e}_{ij} \approx 4\pi\gamma n \int_0^\infty r^2 w_D(r) dr. \tag{22}$$

In many cases, the mass of the system (c^{-1}) goes to zero resulting in a stiff stochastic differential equation. It is of our interest to investigate numerical means to integrate (16).

The system (16), for a constant c, has an integrating factor $\exp\left(ct\right)$, which may be integrated from

$t \to t + \Delta t$

$$e^{c(t+\Delta t)} u\left(t+\Delta t\right) = e^{ct} u\left(t\right) + e^{ct} \int_0^{\Delta t} e^{c\tau} \left(a\left(t+\tau\right) + b\left(t+\tau\right) \theta\left(t+\tau\right)\right) d\tau,$$

to yield the displacement $u\left(t+\Delta t\right)$ at the next time step $t+\Delta t$,

$$u\left(t+\Delta t\right) = e^{-c\Delta t} u\left(t\right) + \Delta A + \Delta B, \tag{23}$$

where

$$\Delta A\left(t;\Delta t\right) = e^{-c\Delta t} \int_0^{\Delta t} e^{c\tau} a\left(t+\tau\right) d\tau, \tag{24}$$

is the forcing function, and

$$\Delta B\left(t;\Delta t\right) = e^{-c\Delta t} \int_0^{\Delta t} e^{c\tau} b\left(t+\tau\right) \theta\left(t+\tau\right) d\tau, \tag{25}$$

is an O-U process. Different integration schemes result from different ways that the integrands in (24)-(25) are approximated.

2.1 First-Order SETD Scheme

First we explore the treatment in which $a = a\left(t\right)$ and $b = b\left(t\right)$ are regarded as constants in the interval $\left(t, t+\Delta t\right)$. In this case

$$\Delta A = \Delta A_1\left(t;\Delta t\right) = e^{-c\Delta t} \int_0^{\Delta t} e^{c\tau} a\left(t+\tau\right) d\tau = \frac{a\left(t\right)}{c} \left(1 - e^{-c\Delta t}\right), \tag{26}$$

and

$$\begin{aligned} \Delta B\left(t;\Delta t\right) &= e^{-c\Delta t} b\left(t\right) \int_0^{\Delta t} e^{c\tau} \theta\left(t+\tau\right) d\tau \\ &= b\left(t\right) \Delta W_1, \end{aligned} \tag{27}$$

where ΔW_1 is the O-U process,

$$\Delta W_1\left(\Delta t\right) = e^{-c\Delta t} \int_0^{\Delta t} e^{c\tau} \theta\left(t+\tau\right) d\tau, \tag{28}$$

with zero mean,

$$\langle \Delta W_1(\Delta t) \rangle = 0, \tag{29}$$

and auto-correlation function

$$\begin{aligned} \langle \Delta W_1(\Delta t)\, \Delta W_1(\Delta t) \rangle &= e^{-2c\Delta t} \int_0^{\Delta t} dt' \int_0^{\Delta t} dt'' e^{ct'} \langle \theta(t+t')\, \theta(t+t'') \rangle e^{ct''} \\ &= \frac{1}{2c}\left(1 - e^{-2c\Delta t}\right). \end{aligned} \tag{30}$$

We call the resulting scheme (23), with (26) and (27) the first-order stochastic exponential time differencing (1st SETD) scheme. In summary, the scheme is defined as

$$u(t+\Delta t) = e^{-c\Delta t} u(t) + \Delta A_1(t;\Delta t) + b(t)\, \Delta W_1(\Delta t), \tag{31}$$

The O-U process $\Delta W_1 = \sqrt{(1 - e^{-2c\Delta t})/2c}\xi$ can be written in terms of a Gaussian distributed process ξ with zero mean and unit mean square as indicated.

2.2 Second-Order SETD Scheme

We next explore a scheme whereby a and b are approximated as linear functions in the interval $0 < \tau < \Delta t$:

$$\begin{aligned} a(t+\tau) &= a(t) + \tfrac{\tau}{\Delta t}\left(a(t) - a(t-\Delta t)\right) = a(t) + \tfrac{\Delta a}{\Delta t}\tau, \\ b(t+\tau) &= b(t) + \tfrac{\tau}{\Delta t}\left(b(t) - b(t-\Delta t)\right) = b(t) + \tfrac{\Delta b}{\Delta t}\tau, \end{aligned}$$

where $\Delta a = a(t) - a(t-\Delta t)$ and $\Delta b = b(t) - b(t-\Delta t)$ are the first-order backward differences for a and b. Then, from (24)

$$\begin{aligned} \Delta A(t;\Delta t) &= e^{-c\Delta t} \int_0^{\Delta t} e^{c\tau} a(t+\tau)\, d\tau \\ &= \frac{a(t)}{c}\left(1 - e^{-c\Delta t}\right) + \frac{\Delta a}{\Delta t} e^{-c\Delta t} \int_0^{\Delta t} e^{c\tau} \tau d\tau \\ &= \Delta A_1(t;\Delta t) + \frac{c\Delta t - 1 + e^{-c\Delta t}}{c^2} \frac{\Delta a}{\Delta t} \\ &= \Delta A_1(t;\Delta t) + \Delta A_2(t;\Delta t), \end{aligned} \tag{32}$$

where $\Delta A_1(t;\Delta t)$ has been defined in (26) and

$$\Delta A_2(t;\Delta t) = \frac{c\Delta t - 1 + e^{-c\Delta t}}{c^2}\frac{\Delta a}{\Delta t}. \tag{33}$$

In addition $\Delta B(t;\Delta t)$ can be integrated as

$$\begin{aligned}\Delta B(t;\Delta t) &= e^{-c\Delta t}\int_0^{\Delta t} e^{c\tau} b(t+\tau)\,\theta(t+\tau)\,d\tau \\ &= b(t)\,\Delta W_1 + \frac{\Delta b}{\Delta t}e^{-c\Delta t}\int_0^{\Delta t}\tau e^{c\tau}\theta(t+\tau)\,d\tau \\ &= b(t)\,\Delta W_1 + \frac{\Delta b}{\Delta t}\Delta W_2,\end{aligned} \tag{34}$$

where the O-U process ΔW_1 has been defined in (28), and the O-U process ΔW_2 is defined as

$$\Delta W_2(\Delta t) = e^{-c\Delta t}\int_0^{\Delta t}\tau e^{c\tau}\theta(t+\tau)\,d\tau. \tag{35}$$

It has zero mean

$$\langle \Delta W_2(\Delta t)\rangle = 0, \tag{36}$$

and its mean square is given by

$$\begin{aligned}\langle \Delta W_2(\Delta t)\Delta W_2(\Delta t)\rangle &= e^{-2c\Delta t}\int_0^{\Delta t}dt'\int_0^{\Delta t}dt''t'e^{ct'}\langle\theta(t+t')\,\theta(t+t'')\rangle\, e^{ct''}t'' \\ &= \frac{1}{4c^3}\left[2c^2\Delta t^2 - 2c\Delta t + 1 - e^{-2c\Delta t}\right].\end{aligned} \tag{37}$$

These estimates result in an integration scheme that we call the second-order stochastic exponential time differencing (2nd SETD) scheme. It is summarised as

$$\begin{aligned}u(t+\Delta t) &= e^{-c\Delta t}u(t) + \Delta A_1(t;\Delta t) + \frac{c\Delta t - 1 + e^{-c\Delta t}}{c^2}\frac{\Delta a}{\Delta t}(t;\Delta t) \\ &\quad + b(t)\,\Delta W_1(\Delta t) + \frac{\Delta b}{\Delta t}\Delta W_2(\Delta t).\end{aligned} \tag{38}$$

The O-U process ΔW_2 can be again expressed in terms of a Gaussian process ξ, of zero mean and unit mean square, as $\Delta W_2 = \sqrt{\left(2c^2\Delta t^2 - 2c\Delta t + 1 - e^{-2c\Delta t}\right)/c}\,\xi/2c$.

2.3 Modified SETD Scheme

In the case of 1st SETD, it is possible to enhance its performance through modifying the autocorrelation function (30). We are motivated by the need of having a slightly lower autocorrelation function for ΔW_1 at large time step Δt (but still keeping $c\Delta t < 1$). This may be achieved by letting

$$\kappa(\Delta t) = \frac{1 - e^{-c\Delta t}}{1 + e^{-c\Delta t}} \frac{2}{c\Delta t}, \tag{39}$$

and then define the following O-U process ΔW_1^*, with autocorrelation function

$$\left\langle \Delta W_1^* (\Delta t)\, \Delta W_1^* (\Delta t) \right\rangle = \kappa(\Delta t) \left\langle \Delta W_1 (\Delta t)\, \Delta W_1 (\Delta t) \right\rangle = \frac{\left(1 - e^{-c\Delta t}\right)^2}{c^2 \Delta t}. \tag{40}$$

Both O-U processes ΔW_1 and ΔW_1^* have identical autocorrelation functions at low $c\Delta t$; at large $c\Delta t$ (but less than unity), ΔW_1^* has slightly reduced autocorrelation function, which makes the calculations more robust and more accurate, a fact borne out by our numerical experiments. In effect, we have numerically approximated the O-U process ΔW_1 by ΔW_1^* in this modified SETD scheme.

Since Equation (16) possesses a relaxation time of $1/c$, one should choose the time step satisfying the condition $c\Delta t < 1$. Figure 1 shows the variation of κ against $c\Delta t$. The curve appears to stay constant ($\kappa = 1$) for $10^{-10} \leq c\Delta t \leq \bar{t}$ and then decreases somewhat for $\bar{t} < c\Delta t < 1$ ($\bar{t} \approx 5 \times 10^{-2}$).

Figure 2 shows the variation of the new and original autocorrelation functions against $c\Delta t$ at $c = 500$. The autocorrelation function $\langle \Delta W (\Delta t)\, \Delta W (\Delta t) \rangle$ obtained by the Wiener process (Brownian motion) is also included. It can be seen that

- When the time step is reduced, the three curves approach together and become indistinguishable from each other for $c\Delta t < 2 \times 10^{-2}$. Alternatively, using power series expansions, we have

$$\left\langle \Delta W (\Delta t)\, \Delta W (\Delta t) \right\rangle = \Delta t, \tag{41}$$

$$\left\langle \Delta W_1 (\Delta t)\, \Delta W_1 (\Delta t) \right\rangle = \Delta t - c\Delta t^2 + (8/12) c^2 \Delta t^3 + O(\Delta t^4), \tag{42}$$

$$\left\langle \Delta W_1^* (\Delta t)\, \Delta W_1^* (\Delta t) \right\rangle = \Delta t - c\Delta t^2 + (7/12) c^2 \Delta t^3 + O(\Delta t^4). \tag{43}$$

- At large time steps, the modified autocorrelation function has slightly lower values than the original autocorrelation, which are both much smaller than that by the Wiener process (Brownian motion).

For the modified one, the stochastic differential equation (31) reduces to

$$u\left(t+\Delta t\right)=e^{-c\Delta t}u\left(t\right)+\left(a+\frac{b\xi}{\sqrt{\Delta t}}\right)\frac{1-e^{-c\Delta t}}{c}, \tag{44}$$

and in addition, we expect that further larger time steps can be used.

3 Numerical results

We first check our algorithms and computer codes through the analytic solution of a geometric Brownian motion, and then test 1st SETD and its modification against the velocity-Verlet scheme [5] in some viscometric flows. Hereafter, we assume identical mass $m_i = m$.

3.1 Geometric Brownian motion

This process is described by the following stochastic differential equation

$$\begin{aligned} dX(t)+cX(t) &= \alpha X(t)dW(t), & (45)\\ X(0) &= X_0. & (46) \end{aligned}$$

The exact solution can be verified to be

$$X(t)=X_0\exp\left[-(c+\frac{1}{2}\alpha^2)t+\alpha W(t)\right]. \tag{47}$$

We conduct the simulation using $\alpha = 1$, $X_0 = 1$ and two large values of c, namely 10 and 100, at $\Delta t = 0.0001$. For all cases, a same set of random numbers over the time domain $0 \leq t \leq 1$ is employed. Figure 3 shows profiles of the exact and computed solutions. It can be seen that the three approximate solutions are indistinguishable from the exact one. A closer look at a part of

the solution for the case of $c = 10$ shows very small discrepancies between the approximate curves, especially for 1st SETD and its modification. On the other hand, 1st SETD and its modification are much more economic than 2nd SETD. At each time level, one needs to evaluate only three terms for 1st SETD, two terms for its modification, but up to 5 terms for 2nd SETD. The corresponding elapsed CPU times are 0.0019, 0.0017 and 0.0050 seconds, respectively (Intel CPU 2.40 GHz). Furthermore, 2nd SETD requires an extra storage space to keep the value of X at $t - \Delta t$. Apart from these, the time step used in the DPD method should be much smaller than the following time scale [3]

$$t_c = \frac{r_c}{V} = \frac{\sqrt{m} r_c}{\sqrt{3 k_B T}} \approx O(\sqrt{m}), \tag{48}$$

where V is the peculiar velocity. It implies that the maximum allowance time step decreases as the particle's mass is reduced, and the use of constant approximations over small time steps (i.e. 1st SETD and its modification) for low-mass DPD systems appears to be appropriate. For these reasons, in simulating fluid flows by means of DPD, 1st SETD and its modification are preferred options. Hereafter, they are denoted by SETD and MSETD, respectively.

3.2 Viscometric flows

We next consider Couette and Poiseuille flows, where analytic solutions are available. The flow domain is chosen as $L_x \times L_y \times L_z = 40 \times 10 \times 30$. We impose periodic boundary conditions in the x and y directions and non-slip conditions at the two planes $z = \pm 15$. The latter is achieved using frozen particles at the wall region and in addition, a thin boundary layer in which a random velocity distribution with zero mean is enforced [4]. Furthermore, the particles are required to leave the wall according to the reflection law proposed in [18]. The motion of a fluid is driven by applying velocity vectors $(\pm 7.5, 0, 0)^T$ to particles in the two thin boundary layers at $z = \pm 15$ for Couette flow and by applying an external force vector $(0.1, 0, 0)^T$ to each particle inside the simulation domain for Poiseuille flow.

We conduct the simulation for two small values of mass, namely 0.1 and 0.01. Other DPD parameters used are $r_c = 1$, $a_{ij} = 18.5$, $\sigma = 3$, $k_B T = 1$, $n = 4$ and $s = 1/2$.

Results concerning the system temperature are presented in Tables 1 and 2 for Couette flow and

in Tables 3 and 4 for Poiseuille flow. For both flows, the present SETD and MSETD schemes outperform the velocity-Verlet algorithm. Much larger values of time step can be employed with SETD and MSETD than with the standart velocity-Verlet algorithm. The velocity-Verlet algorithm fails to give a convergent solution at $\Delta t \gtrapprox 0.009$ and $\Delta t \gtrapprox 0.0009$ for $m = 0.1$ and $m = 0.01$, respectively. In terms of maintaining the equipartition principle, at a given small time step for which the velocity-Verlet algorithm works, the ETD schemes yield the system temperature that is in better agreement with the specified one, *i.e.,* $k_B T = 1$, than the velocity-Verlet algorithm. For $m = 0.1$ and with all time-steps considered, MSETD provides a solution whose error is quite small (less than 0.3% for Couette flow and 0.5% for Poiseuille flow), always smaller than those produced by SETD, and slightly fluctuating with time step (Tables 1 and 3). This fluctuating behavior is probably due to the fact that the use of double-precision floating-point format may prevent the method from achieving lower errors. For all cases, it can be seen that there is an improvement of MSETD over SETD in the satisfaction of equipartition at a given time step. This enhancement in the time-step size is attributed to the fact that the autocorrelation of the fluctuating part of MSETD is slightly reduced at large time steps.

Results concerning the velocity field are presented in Figures 5 and 6 for Couette and Poiseuille flows, respectively. It can be seen that profiles of linear and parabolic velocity are obtained. These figures also show uniform distributions of the number density and temperature.

4 Concluding remarks

This paper reports some new integration schemes, which are based on the method of exponential-time differencing and the Ornstein-Uhlenbeck process, for solving the DPD at low mass overdamped limit. Salient features of the present schemes include (i) they do not contain unwanted fast time scale associated with the stiff part and (ii) the autocorrelation of the fluctuating part has a very slow variation at the high-end time-step region (*i.e.,* $c\Delta t \to 1$). These special features are particularly suitable for the handling of overdamped systems.

Acknowledgement

We would like to thank the Referee for providing helpful comments and suggestions. This work is supported by The Agency for Science, Technology and Research (A*STAR) through grant #102 164 0145. N. Mai-Duy also would like to thank the Australian Research Council for an ARC Future Fellowship.

References

1. S. Chen, N. Phan-Thien, B.C. Khoo, X. Fan, Phys. Fluids 18(10) (2006) 103605.
2. P. Español, Phys. Rev. E 52 (1995) 1734.
3. P. Español, P. Warren, Europhysics Letters 30(4) (1995) 191.
4. X. Fan, N. Phan-Thien, S. Chen, X. Wu, T.Y. Ng, Phys. Fluids 18(6) (2006) 063102.
5. R.D. Groot, P.B. Warren, J. Chem. Phys. 107 (1997) 4423.
6. P.J. Hoogerbrugge, J.M.V.A. Koelman, Europhysics Letters 19(3) (1992) 155.
7. Y. Kong, C.W. Manke, W.G. Madden, A.G. Schlijper, J. Chem. Phys. 107 (1997) 592.
8. C.A. Marsh, G. Backx, M.H. Ernst, Phys. Rev. E 56(2) (1997) 1676.
9. W. Pan, B. Caswell, G.E. Karniadakis, Langmuir 26(1) (2010) 133.
10. I. Vattulainen, M. Karttunen, G. Besold, J.M. Polson, J. Chem. Phys. 116 (2002) 3967.
11. T. Shardlow, SIAM J. Sci. Comp. 24 (2003) 1267.
12. C. Marsh, Theoretical aspects of dissipative particle dynamics, D.Phil thesis, University of Oxford, 1998.
13. D. Pan, N. Phan-Thien, N. Mai-Duy and B.C. Khoo, J. Comput. Phys. 242 (2013) 196.
14. N. Mai-Duy, D. Pan, N. Phan-Thien, B.C. Khoo, J. of Rheology 57(2) (2013) 585.
15. N. Mai-Duy, N. Phan-Thien, B.C. Khoo, J. Comput. Phys. 245 (2013) 150.
16. S.M. Cox, P.C. Matthews, J. Comput. Phys. 176(2) (2002) 430.
17. G.E. Uhlenbeck, L.S. Ornstein, Physical Review 36 (1930) 823.
18. M. Revenga, I. Zúñiga, P. Español, Int. J. Mod. Phys. C 9 (1998) 1319.

Table 1: Couette flow: Comparison of the mean equilibrium temperature of the SETD, MSETD and velocity-Verlet algorithms for the case of $m = 0.1$. The velocity-Verlet algorithm fails to converge at $\Delta t \gtrapprox 0.009$.

	velocity-Verlet		SETD		MSETD	
Δt	$\langle k_B T \rangle$	Error(%)	$\langle k_B T \rangle$	Error(%)	$\langle k_B T \rangle$	Error(%)
0.01	-	-	1.0898	8.98	1.0027	0.27
0.009	-	-	1.0727	7.27	1.0019	0.19
0.007	0.9538	4.62	1.0444	4.44	1.0015	0.15
0.005	0.9386	6.14	1.0240	2.40	1.0019	0.19
0.003	0.9607	3.93	1.0104	1.04	1.0022	0.22
0.001	0.9869	1.31	1.0027	0.27	1.0018	0.18
0.0009	0.9884	1.16	1.0024	0.24	1.0019	0.19

Table 2: Couette flow: Comparison of the mean equilibrium temperature of the SETD, MSETD and velocity-Verlet algorithms for the case of $m = 0.01$. The velocity-Verlet and SETD algorithms fail to converge at $\Delta t \gtrapprox 0.0009$ and $\Delta t \gtrapprox 0.0005$, respectively.

	velocity-Verlet		SETD		MSETD	
Δt	$\langle k_B T \rangle$	Error(%)	$\langle k_B T \rangle$	Error(%)	$\langle k_B T \rangle$	Error(%)
0.005	-	-	-	-	0.7633	23.66
0.003	-	-	1.5963	59.63	0.9356	6.44
0.001	-	-	1.0689	6.89	0.9835	1.64
0.0009	-	-	1.0559	5.59	0.9863	1.36
0.0007	0.9187	8.12	1.0341	3.41	0.9916	0.83
0.0005	0.9322	6.77	1.0178	1.78	0.9958	0.41
0.0003	0.9576	4.23	1.0066	0.66	0.9987	0.12
0.0001	0.9840	1.60	1.0000	0.00	0.9992	0.07

Table 3: Poiseuille flow: Comparison of the mean equilibrium temperature of the SETD, MSETD and velocity-Verlet algorithms for the case of $m = 0.1$. The velocity-Verlet algorithm fails to converge at $\Delta t \gtrapprox 0.009$.

	velocity-Verlet		SETD		MSETD	
Δt	$\langle k_B T \rangle$	Error(%)	$\langle k_B T \rangle$	Error(%)	$\langle k_B T \rangle$	Error(%)
0.01	-	-	1.0915	9.15	1.00418	0.42
0.009	-	-	1.0745	7.45	1.00348	0.35
0.007	0.9558	4.42	1.0462	4.62	1.00295	0.30
0.005	0.9399	6.01	1.0254	2.54	1.00317	0.32
0.003	0.9614	3.85	1.0115	1.15	1.00339	0.34
0.001	0.9875	1.24	1.0034	0.34	1.00258	0.26
0.0009	0.9891	1.09	1.0029	0.29	1.00239	0.24

Table 4: Poiseuille flow: Comparison of the mean equilibrium temperature of the SETD, MSETD and velocity-Verlet algorithms for the case of $m = 0.01$. The velocity-Verlet and SETD algorithms fail to converge at $\Delta t \gtrapprox 0.0009$ and $\Delta t \gtrapprox 0.0005$, respectively.

	velocity-Verlet		SETD		MSETD	
Δt	$\langle k_B T \rangle$	Error(%)	$\langle k_B T \rangle$	Error(%)	$\langle k_B T \rangle$	Error(%)
0.005	-	-	-	-	0.76248	23.75
0.003	-	-	1.59533	59.53	0.93494	6.50
0.001	-	-	1.06904	6.90	0.98353	1.64
0.0009	-	-	1.05609	5.60	0.98647	1.35
0.0007	0.9190	8.09	1.03424	3.42	0.99158	0.84
0.0005	0.9321	6.78	1.01797	1.79	0.99585	0.41
0.0003	0.9574	4.25	1.00679	0.67	0.99878	0.12
0.0001	0.9843	1.56	1.00008	0.00	0.99887	0.11

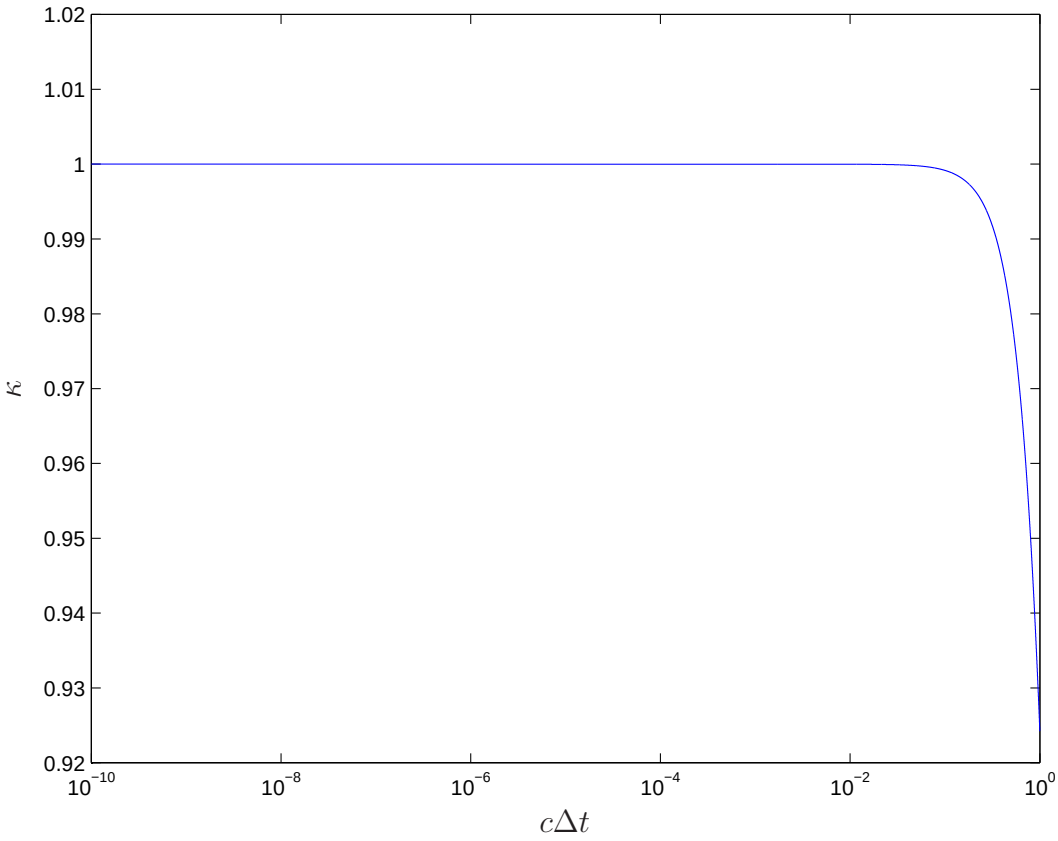

Figure 1: A modification function.

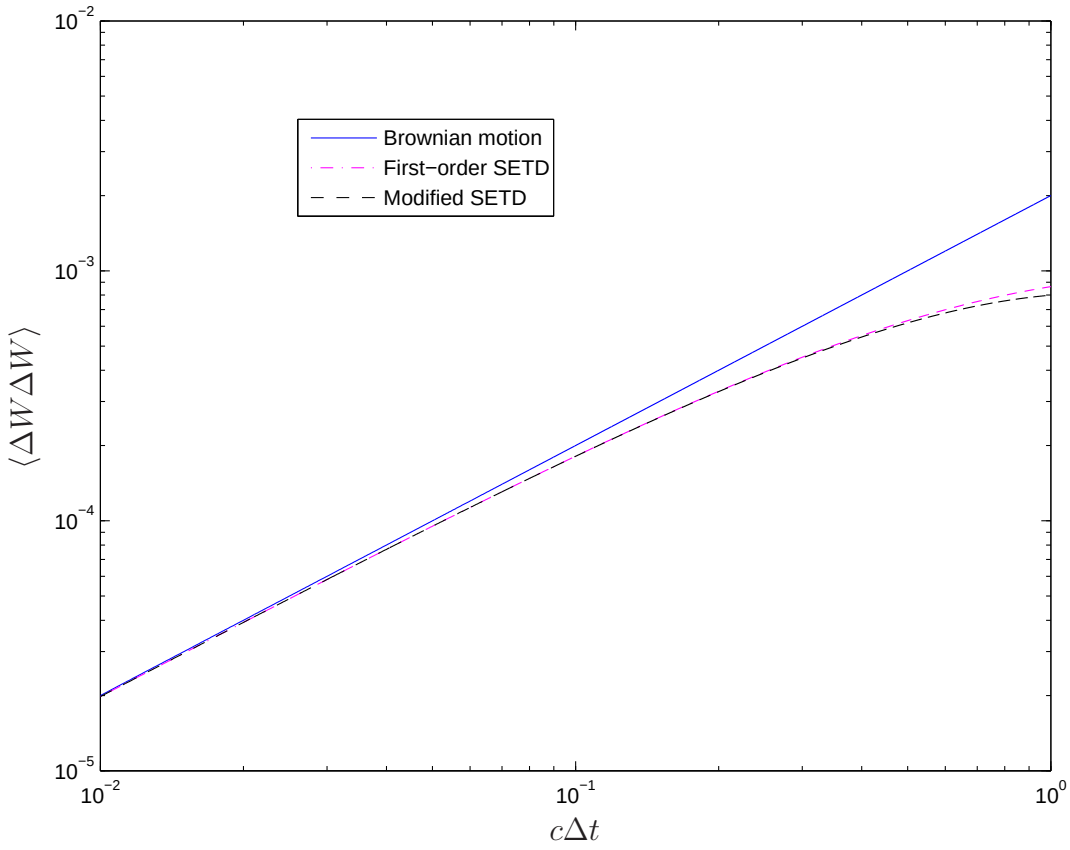

Figure 2: Variations of the autocorrelation function by several approaches.

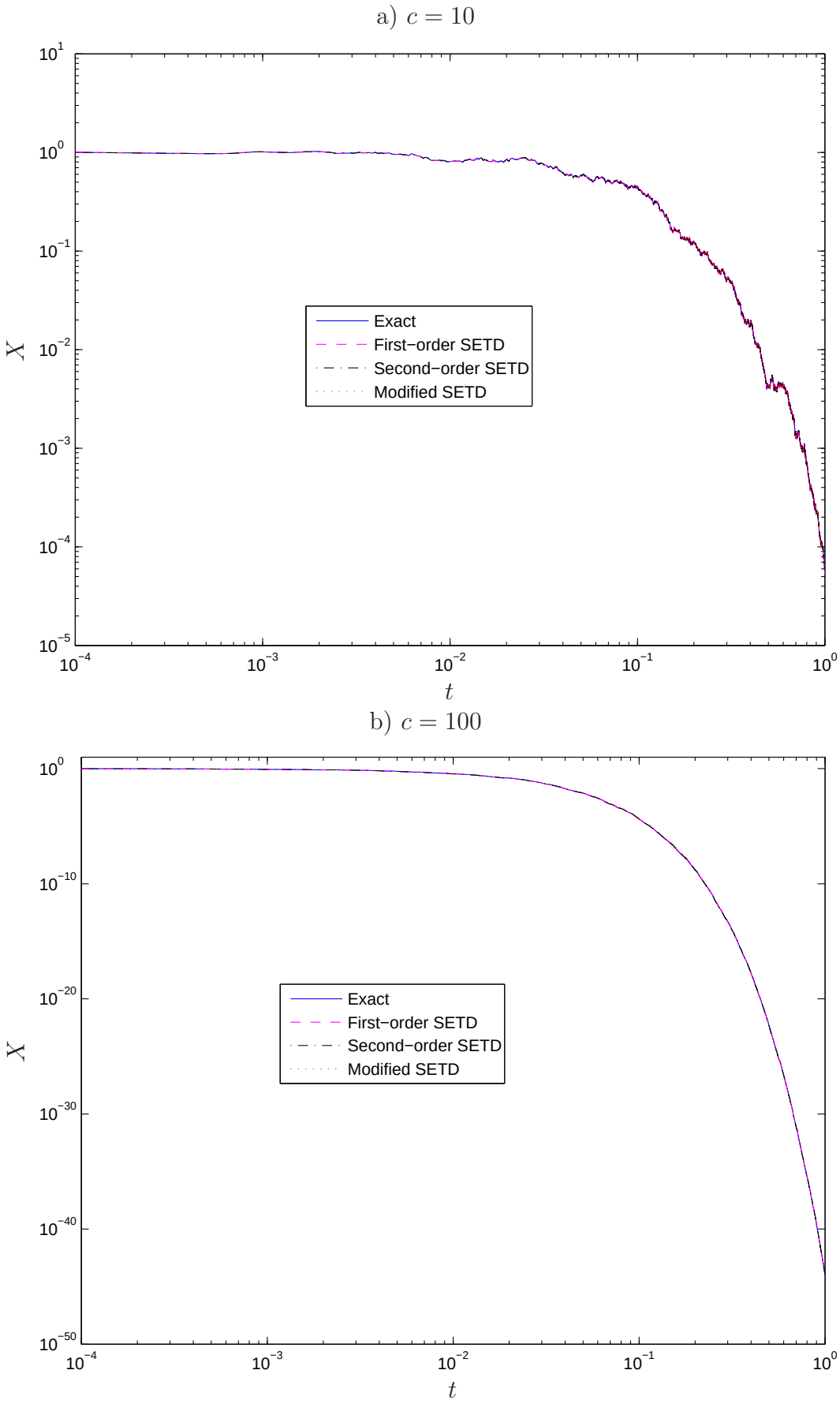

Figure 3: Geometric Brownian motion: Profiles of the exact and approximate solutions for two values of c.

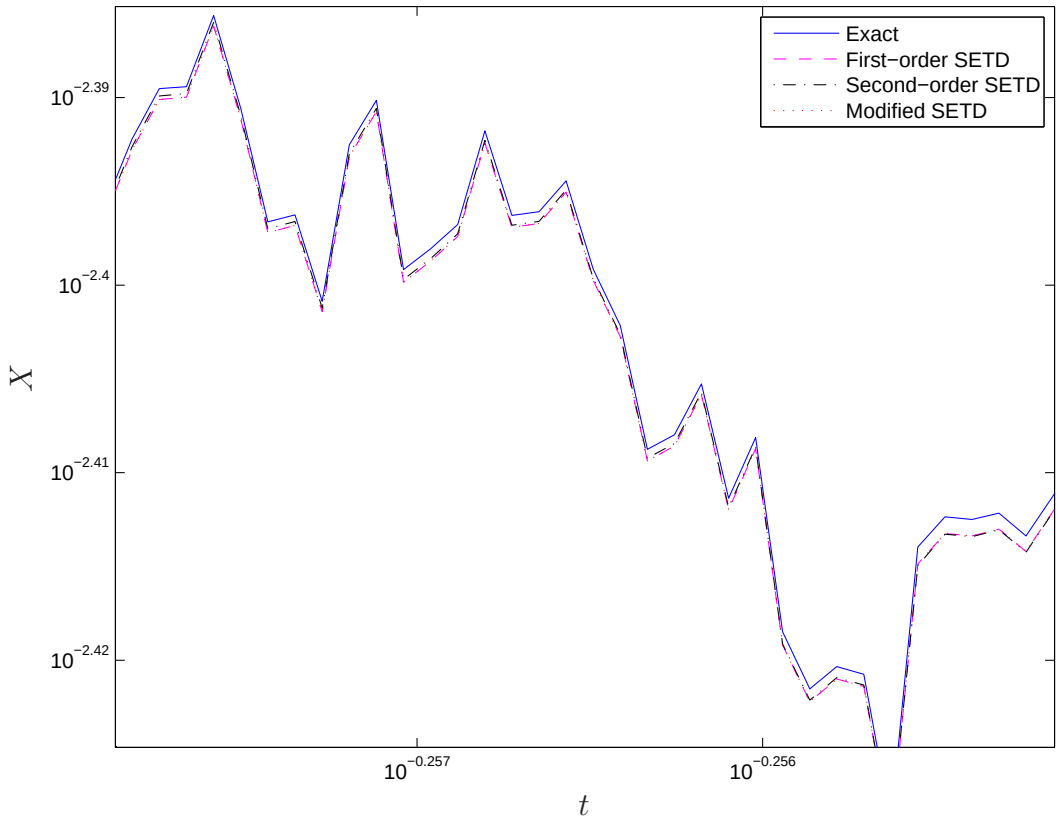

Figure 4: Geometric Brownian motion: A closer look at a part of the solution curve for the case of $c = 10$.

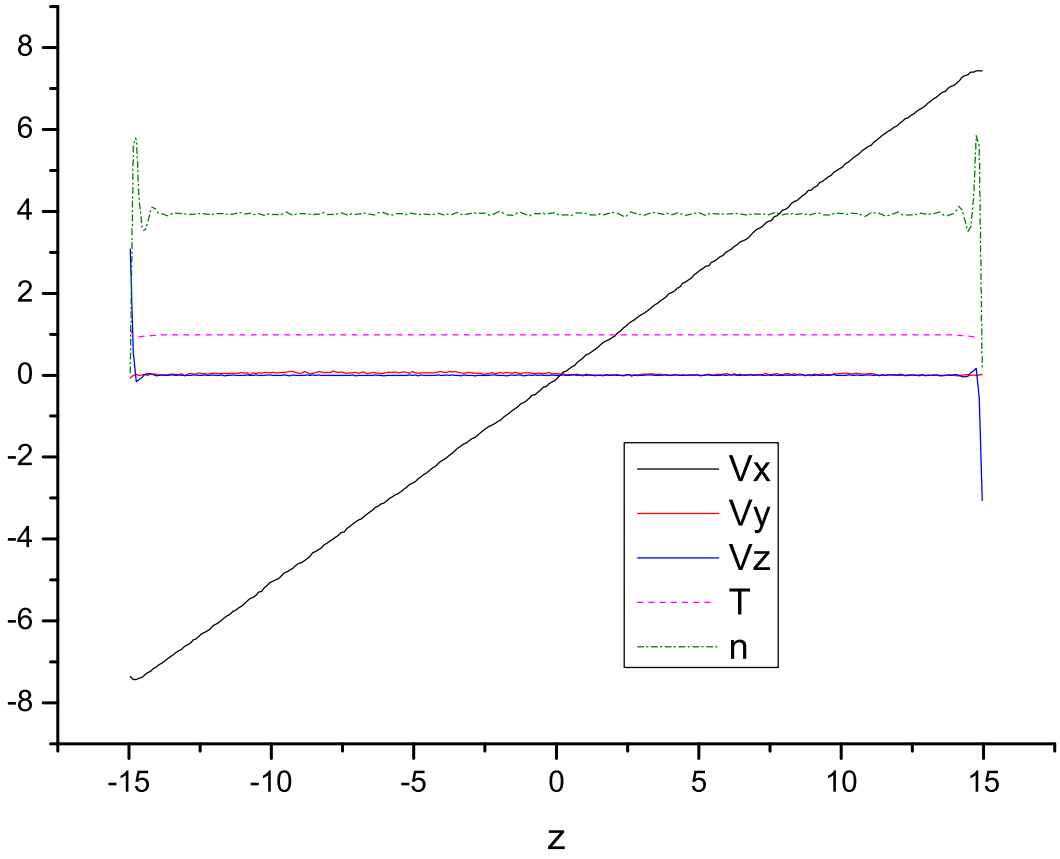

Figure 5: Coutte flow, $m = 0.01$, $\Delta t = 0.001$: Profiles of the velocity, temperature and number density by MSETD.

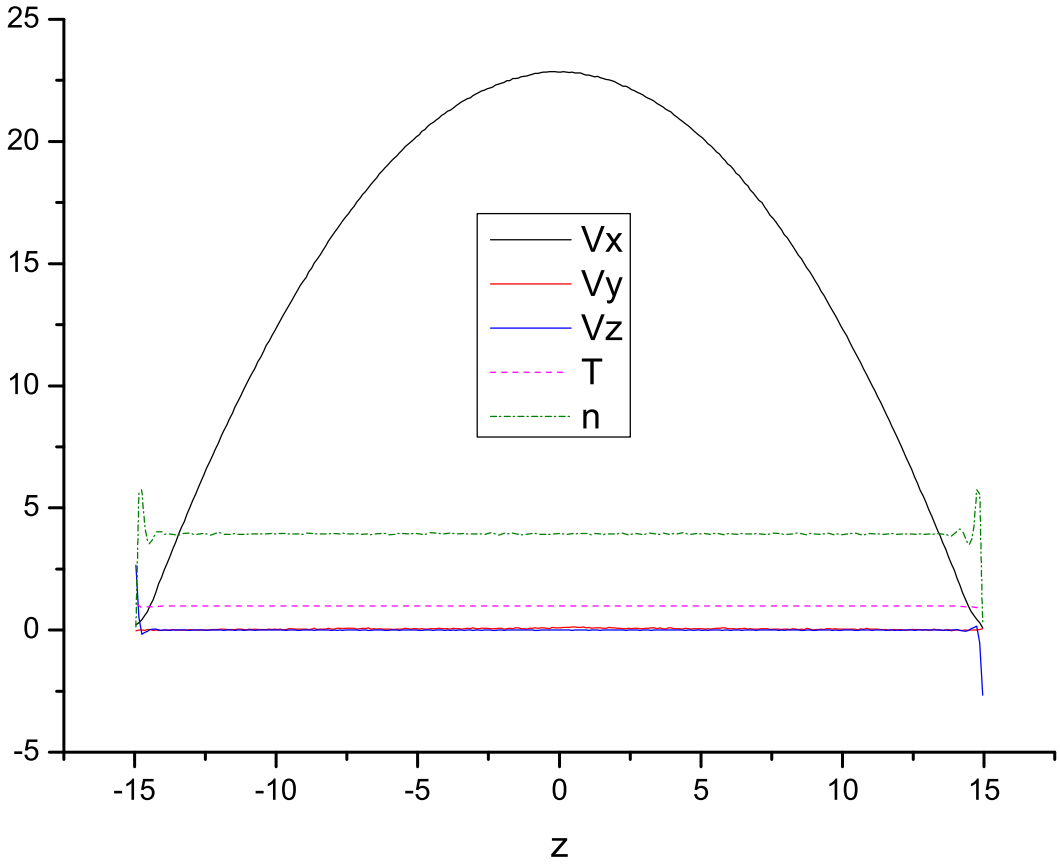

Figure 6: Poiseuille flow, $m = 0.01$, $\Delta t = 0.001$: Profiles of the velocity, temperature and number density by MSETD.